



RESEARCH ARTICLE

## Assessment of Pollution and Identification of Sources of Heavy Metals, and Radionuclides Contamination in Sand along the Southern Part of the Cameroonian Coast (South-West, Africa)

Francis Temgo Sopie<sup>1</sup> Victorine Ambassa Bela<sup>2</sup> Armel Zacharie Ekoa Bessa<sup>2\*</sup> Archange Duviol Tsanga<sup>2</sup>  
Patrice Roland Liyouck<sup>1</sup> Théophile Njanko<sup>1</sup> Gabriel Ngueutchoua<sup>2</sup>

1. Department of Earth Sciences, University of Dschang, Dschang, Cameroon

2. Department of Earth Sciences, University of Yaoundé I, Yaoundé, Cameroon

---

ARTICLE INFO

*Article history*

Received: 15 April 2022

Revised: 19 May 2022

Accepted: 24 May 2022

Published Online: 2 June 2022

*Keywords:*

Pollution indices

Statistical analysis

Ecological risk

Heavy metals and radionuclides

Source identification

---

ABSTRACT

Sandy sediments collected along the southern part of the Cameroonian coast have been analyzed geochemically by ICP MS methods to investigate the distribution characteristics, contamination levels and related ecological risks. In these sediments, the concentration (mg/kg) of selected elements are in order Fe > Mn > Cr > V > Th > Ni > U > Co. Indices of pollution such as index of geoaccumulation, where values of all elements in the sediments were < 0, except Th in the sediments station of Yoyo II, and Cr in sediment of all stations were Igeo > 0. The contamination factor shows that the station of Yoyo II has values of CF < 1, such as Fe, V, Ni and Co. While Uranium, Th and Mn values vary from 1 to 3 and 3 to 6, and for Cr values of CF > 6. However, Kribi and Campo stations show that all the elements have values of CF < 1, except Cr which has values of CF > 6. The degree of contamination values ranges between (9.48-37.13) for the station of Yoyo II, (8.84-17.62) for the Kribi station, and (6.52-13.56) for the Campo station. The pollution loading index values at all sampling stations are lower than 1. The potential ecological risk (Er and RI), indicates that this coastal area is a low risk region. Pearson correlation, cluster analysis and principal component analysis supported that heavy metals (Fe, Mn, Cr, V, Ni and Co) have common human influences while radionuclides (Th and U) have a natural source. The presence of human activities such as domestic waste, intensive farming and the processing of industrial products could be potential sources of anthropogenic environmental pollution, thereby threatening the environmental concerns of the entire study area.

---

\*Corresponding Author:

Armel Zacharie Ekoa Bessa,

Department of Earth Sciences, University of Yaoundé I, Yaoundé, Cameroon;

Email: [armelekoa@yahoo.fr](mailto:armelekoa@yahoo.fr)

DOI: <http://dx.doi.org/10.36956/eps.v1i1.525>

Copyright © 2022 by the author(s). Published by Nan Yang Academy of Sciences Pte. Ltd. This is an open access article under the Creative Commons Attribution-NonCommercial 4.0 International (CC BY-NC 4.0) License (<https://creativecommons.org/licenses/by-nc/4.0/>).

## 1. Introduction

Over the past two decades, pollution of aquatic sediments has become a worldwide environmental concern<sup>[1]</sup>. Heavy metals in deposition persist in the environments, which poses a risk, not only to benthic but also to aquatic biota, as metals in sediments can be discharged into the aquatic overlying waters through both chemical and biological processes<sup>[2,3]</sup>. The characteristics and behavior of coastal habitats are diverse and changing. There are sandy beaches, which can be considered as the geographical area where the marine and terrestrial ecological systems interact. Such settings are critical for the survival of a wide range of plants and animals, as well as a wide range of economic activities. In recent years, there has been an increase in global concern about the effects on coastal habitats<sup>[4-6]</sup>. Pollution from industrial activities such as discharges of urban sewage, fishing activities, and the combustion of fossil fuels via the dumping of solid waste has extensively affected the environments throughout the land-linked coastline<sup>[6-8]</sup>. As a result of their highly toxicity, prolonged occurrence, slow rate of degradation, and simple accumulation by marine biota, heavy metals in sediments have received scientific attention and public concern recently<sup>[3,9]</sup>. Metals including Pb, Cd, Zn, Cr, Cu, and Ni are predominantly mobilized by human activity, while other metals like Al, Fe, Co, and Mn are of lithogenic origin<sup>[10]</sup>. Natural radiation has been a part of human life throughout history. Its principal mechanisms are cosmogenic and cosmic gamma radiation, terrestrial gamma radiation from naturally occurring radionuclides in soils, sediments, and rocks, and naturally occurring radioactive constituents in our food and inhaled air<sup>[5,11,12]</sup>. Uranium and thorium are found in fairly low abundances in rocks, soils, and sediments<sup>[5]</sup>. Thorium is a strikingly abundant element in the Earth's crust, almost three times more abundant than uranium<sup>[13]</sup>. Felsic rocks (e.g. granite) have been found to have higher U and Th content than mafic rocks like basalt and andesites<sup>[5,14]</sup>.

Heavy metals in coastal sediments are the result of natural processes and/or anthropogenic activities. The background values for heavy metals are determined by natural processes such as atmospheric input, Aeolian processes, and crustal movements<sup>[3]</sup>. Industrialization and agricultural practices are linked to anthropogenic heavy metals inputs. The major anthropogenic inputs are from sources including atmospheric deposits, waste disposal, waste combustion, urban effluents, traffic emissions, fertilizer application, and long-term application of wastewater to farmland<sup>[4]</sup>. To investigate the source of heavy metals in terrestrial and littoral environments, several factors need to be examined, such as grain size, mineral compo-

sition, and the sedimentary environment. Metals that have leached into sediments from anthropogenic sources, on the other hand, are more commonly present in relatively more bioavailable forms<sup>[15,16]</sup>. Soil erosion, natural weathering of the Earth's crust, mining, industrial effluents, urban runoff, sewage discharge, and pest or disease-control agents are all sources of heavy metals in today's crops<sup>[17,18]</sup>. Therefore, the purposes of the present study were: (i) to determine the spatial distribution of selected heavy metals contents along the Southern part of the Cameroonian coast; (ii) to assess heavy metal contamination levels and potential ecological risk in the study area based on the geo-accumulation index and potential ecological risk; (iii) to definite the possible source of pollutants using multivariate statistical analyses.

## 2. Materials and Methods

### 2.1 Study Area

The area under study is located in the southern part of the Cameroonian coast, near the mouth of the Sanaga River located on the Atlantic Ocean coast, ranging from 2°20' to 3°40' N and 9°40' to 10°20' E in southwestern (SW) Cameroon (Figure 1). The wet season lasts from March to November, and the dry season lasts from December to February. The soils in this area are ferrallitic and hydromorphic<sup>[19]</sup>. The main activities in this area are artisanal fishing and agriculture. The geology of the Cameroonian coast is dominated by sedimentary strata associated with the Douala Basin. From the Upper Cretaceous to the Tertiary, marine transgression has sculpted these strata<sup>[20,21]</sup>. The Douala sub-basin is located in the Gulf of Guinea between the Cameroon Volcanic Line and the Rio Muni basin in Cameroon. According to Nguene et al.<sup>[22]</sup> and Lawrence et al.<sup>[23]</sup>, three major events in geodynamics and sedimentary history can be distinguished: (i) the early Cretaceous extensional rift to drift phase; (ii) the transition from rift to drift highlighted by the accentuation of transformed directions caused by a series of cross faults; and (iii) the late Cretaceous and Tertiary passive margin wedge. The Cameroonian coast is unconformably underlain by the Precambrian basement and begins with a marl and fossiliferous limestone marine series of lower Turonian-Campanian age and is continued by a Campanian-Paleocene continental series to date<sup>[24]</sup>. Also known as the Dizangue series, it is composed of small conglomerates at the base, and fine and coarse sandstones at the top. The series also contains interbedded clay, kaolinite, and ferruginous sandstone<sup>[20,25]</sup>. In the Sanaga upstream basin, there is a succession of fine, black and beige sandstones and Middle Cretaceous arkosic conglomeratic sandstones<sup>[6]</sup>.

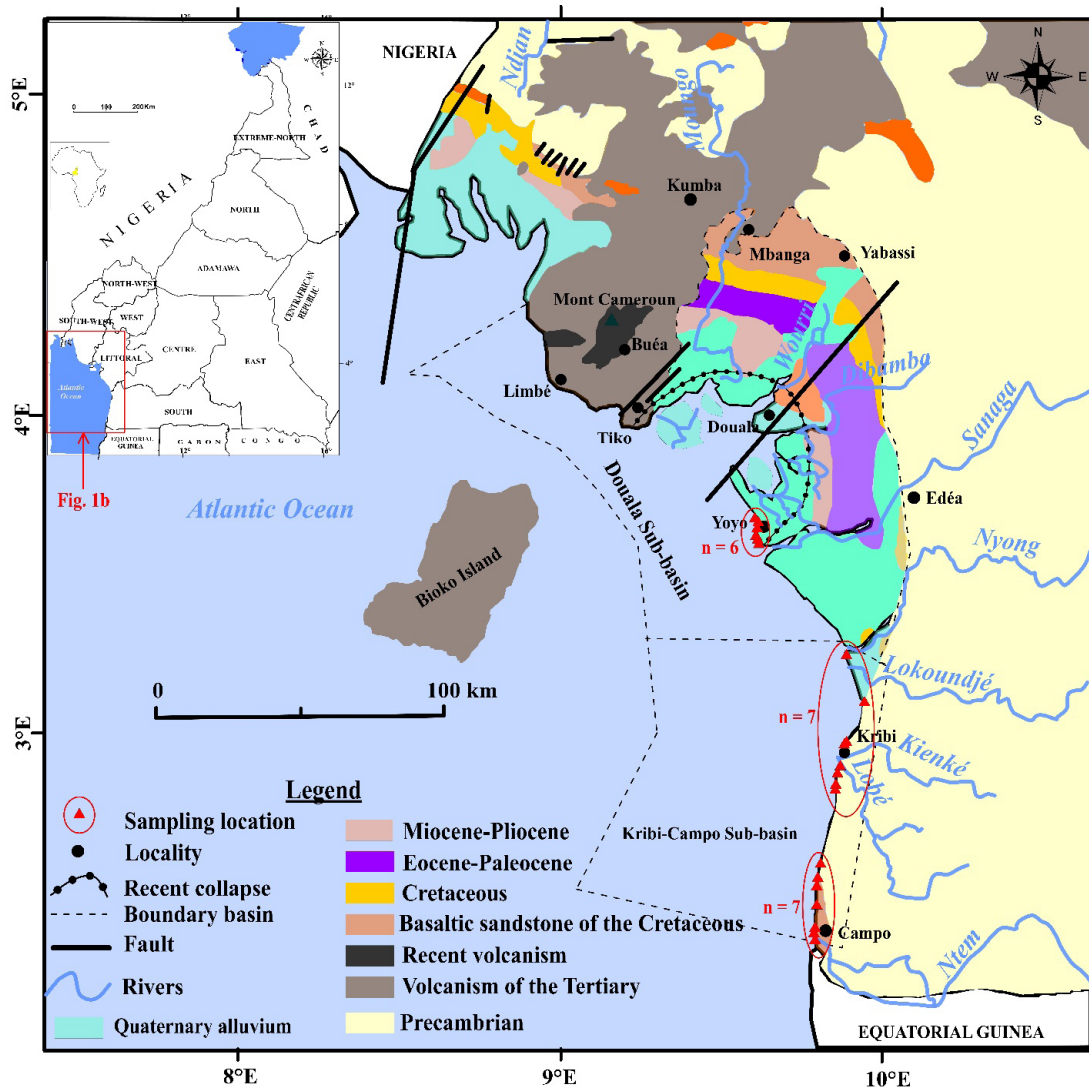


**Figure 1.** Investigated area and sampling location: a) location of the study area and in Cameroon; b) Location of sampling area and station along the southern part of the Cameroonian coast.

## 2.2 Sample Collection and Analysis

The sediments were sampled at three sites, for a total of 20 samples collected, selected according to the type of slope, surroundings and sampling of the sediments and water along the coastal shoreline. The three sites are Yoyo II, Kribi and Campo. Sampling was collected in February 2022, at the designated locations, with the use of a trowel. This one is used to scrape off the top layer 10-15 cm) of sediment to prevent contamination. Polyethylene bags have been used to pack and carry the samples to the laboratory. About 2 kg of each sample was collected. The samples were then air-dried, ground, and then sieved. The ground samples, 0.2 g (ground, sieved with a 0.080 mm) have been prepared and mixed with 1.5 g of LiBO<sub>2</sub>. The mixture was then dissolved in 100 mL of 5% HNO<sub>3</sub>. The metal concentration intensity of Fe, Mn, Cr, V, Ni, Th, U

and Co was determined in air/acetylene fire by inductively coupled plasma mass spectrometry (ICP-MS) from ALS (Australian Laboratory Services), Vancouver, Canada. Analytical doubts ranged from 0.1 to 0.5% for trace metals. The detection limits vary from  $0.05 \times 10^{-6}$  mg/g to  $4.0 \times 10^{-6}$  mg/g according to the element.

The statistical descriptions of heavy metals were obtained from the PAST program (version 1.72). Box and whisker plots of sediment quantification were drawn for the three sites to show the variation in the heavy metal concentrations investigated. Furthermore, the heavy metal data from the three sites were subject to agglomerative hierarchical analysis (AHC) and principal component analysis (PCA) to build a correlation matrix, and to identify if a significant variation between the different treatments exists. The PCA was carried out with the statistical software

package XLSTAT, version 14.

## 2.3 Assessment Methods of Sediment Pollution

### 2.3.1 Geoaccumulation Index (Igeo)

Popular measure to determine the extent of metal deposition in sediments is the geoaccumulation index (Igeo) Chen et al. [26] and Singovszka and Blintova [27]. The Igeo takes into account both the impact of human activities and the background concentration of the area. The index is expressed mathematically as follows:

$$I_{geo} = \log_2 (C_i/k \times B_i) \quad (1)$$

where  $C_i$  denotes the content of element ( $i$ ) in the selected materials,  $B_i$  denotes the geochemical content of element ( $i$ ), and  $k$  is a factor that accounts for probable lithogenic effect variation in background data. Factor  $k$  normally has a value of 1.5. There are six classes on the Igeo scale, varying from unpolluted to very strongly polluted (Table 1).

### 2.3.2 Contamination Factor (CF), Degree of Contamination (DC) and Pollution Load Index (PLI)

The CF is the calculated ratio resulting from the following equation [28].

$$CF = (C_{\text{metal}} / C_{\text{background}}) \quad (2)$$

$C_{\text{metal}}$  is the concentration of pollutants in the deposits and  $C_{\text{background}}$  refers to the background metal concentrations. We classified the CF into four groups to measure the contamination level (Table 1).

The degree of contamination (DC) is the sum of all contamination factors for a given site [29]. The DC can be calculated using the equation:

$$DC = \sum_{i=1}^n CF_i \quad (3)$$

in which CF is the single contamination factor and  $n$  is the element amount present.  $DC < n$ , would denote a low degree of contamination;  $n \leq DC < 2n$ , moderate degree of contamination;  $2n \leq DC < 4n$ , considerable degree of contamination and  $DC > 4n$ , very high degree of contamination. For this studied heavy metals  $n = 8$ .

The pollution load index (PLI) is a combined approach of factors in the studied area [30]. The PLI could indicate temporal and spatial variance, as well as each element's contribution to overall pollution [28]. The pollution load index (PLI) is calculated using an equation from Tomlinson et al. [28].

$$PLI = \sqrt[n]{(CF_1 \times CF_2 \times CF_3 \times \dots \times CF_n)} \quad (4)$$

$n$  is the number of metals, while CF refers to the contamination factor. The pollution loading index was interpreted by Tomlinson et al. [28] and Suresh et al. [31]. The PLI is categorized into three ranks as described in Table 1.

### 2.3.3 Ecological Risk Assessment

For the current study, a prospective ecological risk factor ( $E_r^i$ ) and a possible ecological risk index (RI) were used to estimate the ecological risk. The ecological risk potential is determined using Håkanson [29] technique. The RI was created in order to quantify the extent of trace metals contamination in sediments, as well as their toxicity and environmental impact.

$$E_r^i = Tr \times CF \quad (5)$$

$$RI = \sum_{i=1}^n E_r^i \quad (6)$$

RI denotes the sum of all risk factors for heavy metals in the selected sediment, ( $E_r^i$ ) is the potential monomial environmental risk factor proposed by Håkanson [29] and Suresh et al. [31]; Tr is the toxic response factor proposed by Håkanson [29] for three metals Mn (1), Cr (2), and Ni (5),

**Table 1.** Classes of pollution indices and contamination levels used in the study.

I-geo value ; classes	Pollution level	Er classes	Er level
I-geo ≤ 0 ; 0	Unpolluted	Er < 40	Low potential ecological risk
I-geo = 0-1 ; 1	Unpolluted to moderately polluted	Er = 40-80	Moderate potential ecological risk
I-geo = 1-2 ; 2	Moderately polluted	Er = 80-160	Significant potential ecological risk
I-geo = 2-3 ; 3	Moderately to strongly polluted	Er = 160-320	High potential ecological risk
I-geo = 3-4 ; 4	Strongly polluted	Er > 320	Very high potential ecological risk
I-geo = 4-5 ; 5	Strongly to very strongly polluted		
RI classes	Risk level	CF classes	Contamination level
RI < 150	Low ecological risk	CF < 1	Low contamination
RI = 150-300	Moderate ecological risk	CF = 1-3	Moderate contamination
RI = 300-600	Significant ecological risk	CF = 3-6	Considerable contamination
RI > 600	High ecological risk	CF > 6	High contamination

and CF is the contamination factor determined by Equation (2). The expressions and values used for the ecological risk assessment interpretation are presented in Table 1.

## 2.4 Multivariate Statistical Analyses

The statistical analysis was carried out with Microsoft Excel version 16, whereas Surfer 16 was used to plot the maps. Heavy metals in sediment for each individual habitat were performed in a one-way ANOVA with equal probability replication at the 0.05 level (Duncan's test) by using the program COSTAT 6.3. In this study, multivariate statistical analysis was carried out using Pearson correlation, cluster analysis, and principal component analysis (PCA).

## 3. Results and Discussion

### 3.1 Distribution of Heavy Metals and Radionuclides

The distribution of heavy metals (Fe, Mn, Cr, V, Ni, Co) and radionuclides (Th and U) observed in the beach sand along the Southern part of the Cameroonian coast is presented in (Table 2). The mean concentration (mg/kg) of these elements were found in the following decreasing order as Fe (4755.92-116,450.1) > Mn (77.45-3407.8) > Cr (547.36-957.88) > V (5-318) > Th (0.46-161) > Ni (4-22) > U (0.21-21.9) > Co (1-18) (Table 2). However, all metals are higher than the average Shales values<sup>[32]</sup> except Ni and Co which have lower values (Table 2). Metal concentrations in sediments vary due to changes in bedrock composition, sediment texture, sediment transport, mineral sorting, and anthropogenic activities<sup>[5,33]</sup>. Activities such as runoff from agricultural land, exposure of the Atlantic Ocean to substantial releases of pollutants from industrial processes, and untreated domestic sewage from residential areas may have raised the concentration of these metals in this coastal area<sup>[25]</sup>. The highest concentration of Fe is most likely to be caused by natural processes such as leaching of source rocks, transported from the continent and transported directly from the ocean by rivers and wave movements<sup>[6,25]</sup>. Similarly, increasing Fe concentrations could have been caused by urban and industrial waste, as well as corrosion of underwater structures<sup>[34,35]</sup>. Manganese has been found in a variety of amounts as a natural trace element in crude oils, which has been used to improve fuel oil combustion<sup>[36]</sup>. The average amounts found in this study are attributed to the presence of mangrove vegetation<sup>[6,37]</sup>. The amounts of Cr could be linked to the pollution load resulting from diverse agricultural wastes<sup>[5]</sup>. The occurrence of Cr in this study could be attributed to the combustion of plastic trash, anthropogenic waste dumping, and tourism-related sludge dredging. Vanadium is found in carbon-rich materi-

als like crude oil, coal, oil shale and oil sands. Because V is generally relatively soluble, weathering is an essential way for it to be distributed in the environment. It's found in algae, plants, invertebrates, fish, and a variety of other species. Furthermore, human activities such as marketplaces and garages would be responsible for the high values of V in sands<sup>[6,38]</sup>. Natural weathering and rock leaching can cause Ni to reach the environment<sup>[39]</sup>. Fishing, tourist activities, and rock leaching could all contribute to the moderate Ni concentration. Cobalt is rarely found naturally in the environment. It is usually manufactured as by-product of nickel and copper mining. When Co particles are not attached to soil or sediment particles, however, plant and animal uptake is stronger, and buildup in plants and animals is possible. Furthermore, the significant concentration of Co could be related to the presence of iron and manganese oxyhydroxide in sediments because Co is considered a low mobility element in sediments and has a strong affinity with iron and manganese oxyhydroxide. Thorium is a radioactive element and can be found in low concentrations in most rocks and soils. This element circulates very little in nature due to its high insolubility when it is in the oxide form<sup>[5,40]</sup>. In addition to Th, U is radioactive, but it is not especially rare. It can occur in minor quantities in rocks and sediments, in both water and air, in varying concentrations that are generally very low. However, due to its solubility in water, which determines its mobility in the environment as well as its toxicity, U is unlikely to be found in fish or vegetable products<sup>[5,12,41]</sup>. In this study, high concentrations of U in the sediments would be due to anthropogenic activities such as the use of coal, and phosphate fertilizers in agricultural production.

### 3.2 Geoaccumulation Indices of Heavy Metals and Radionuclides

The geoaccumulation index (Igeo) of the different metals (Fe, Mn, V, Ni, Co) and radionuclides (Th and U) of the sediment samples from Yoyo II, Kribi and Campo are given in Appendix 1. The station of Yoyo II shows that most of the metals contained in the samples have values of Igeo < 0, while Cr and Th have values of Igeo > 0 (Appendix 1; Table 1). The results obtained show that, the sediments of Yoyo II are mostly unpolluted in Fe, Mn, V, Ni, Co and U, and moderately to strongly polluted in Cr and Th (Table 1; Figure 2). The results are similar to those of Chougong et al.<sup>[5]</sup> on the alluvial sediments of the Lobé river in Cameroon. The results obtained in the Kribi and Campo sediment samples are similar for both heavy metals and radionuclides (Th and U). Sediments from these two sites have values of Igeo < 0 in most samples, except for Cr which has values of Igeo > 0 in all samples from

both sites (Appendix 1; Table 1). The sediments of the Kribi and Campo site are all unpolluted in Fe, Mn, V, Ni, Co, Th and U. Moreover, these same samples show that the sediments of Kribi and Campo location are moderately to strongly polluted in Cr (Table 1; Figure 2).

These results corroborate those obtained on beach sediments along the Littoral zone of Cameroon <sup>[6]</sup>. Moreover, these results are far from those obtained on the sediments

of the various beaches of Limbé which shows that, the sediments are polluted in Co, Ni, Cu and Cd on the one hand, and on the other hand unpolluted in Zn, Cr, Fe and Mn <sup>[25]</sup>. The unpolluted nature of sediments in these different sites would be due to the fact that the various anthropogenic activities carried out in these areas do not contribute significantly to the contamination of the sediments. High Cr Igeo values suggest that sediment retains more Cr than other metals <sup>[5,42]</sup>.

**Table 2.** Descriptive statistical of heavy metals and radionuclides concentration (mg/kg).

ID	Fe	Mn	Cr	V	Ni	Co	Th	U	Station
Yo1	21471.58	309.8	615.78	37	9	5	8.9	1.46	Yoyo II
Yo2	40355.38	1084.3	684.2	102	14	7	51.7	7.66	
Yo3	99314.8	2943.1	752.62	272	19	15	150	19.2	
Yo5	28115.88	542.15	821.04	53	11	5	30	4.2	
Yo6	116450.1	3407.8	684.2	318	22	18	161	21.9	
PYo0	16645.72	154.9	752.62	23	9	4	2.9	0.8	
Min	16645.72	154.9	615.78	23	9	4	2.9	0.8	
Max	116450.1	3407.8	821.04	318	22	18	161	21.9	
Mean	53725.58	1407.01	718.41	134.17	14	9	67.42	9.20	
SD	43040.91	1413.26	71.756	128.23	5.44	5.97	70.44	9.16	
Lje	12169.56	154.9	684.2	15	7	3	3.1	0.61	Kribi
Lji	46230.34	1471.55	684.2	156	19	10	40.6	7.11	
Lo2	45181.24	697.05	615.78	72	14	10	8	1.82	
Lo1	17065.36	232.35	752.62	22	7	2	2.4	0.62	
Lb	19862.96	309.8	752.62	24	9	4	4.3	0.9	
EB2	31822.7	542.15	615.78	60	12	6	6.9	1.42	
Eb1	31053.36	232.35	889.46	59	14	6	4.4	1.25	
Min	12169.56	154.9	615.78	15	7	2	2.4	0.61	
Max	46230.34	1471.55	889.46	156	19	10	40.6	7.11	
Mean	29055.07	520.02	713.52	58.29	11.71	5.86	9.96	1.96	
SD	13416.81	461.93	95.60	48.49	4.39	3.18	13.66	2.31	
CD	23709.66	309.8	957.88	30	11	5	3.9	0.87	Campo
CE	41894.06	1084.3	752.62	84	14	8	12.5	2.67	
CRL	48258.6	929.4	684.2	91	17	8	9.9	2.51	
CB1	4755.92	77.45	547.36	5	4	1	0.46	0.21	
CB2	24199.24	309.8	684.2	30	10	5	2.1	0.74	
CV1	27486.42	542.15	821.04	52	10	6	12.6	2.07	
CV2	20282.6	309.8	547.36	28	9	4	10.2	1.15	
Min	4755.92	77.45	547.36	5	4	1	0.46	0.21	
Max	48258.6	1084.3	957.88	91	17	8	12.6	2.67	
Mean	27226.64	508.96	713.52	45.71	10.71	5.29	7.38	1.46	
SD	14330.80	368.35	147.05	31.68	4.07	2.43	5.09	0.95	
Average Shale	47,200	850	90	130	68	19	12	3.7	-

Average shale, after Turekian and Wedepohl <sup>[5]</sup>.

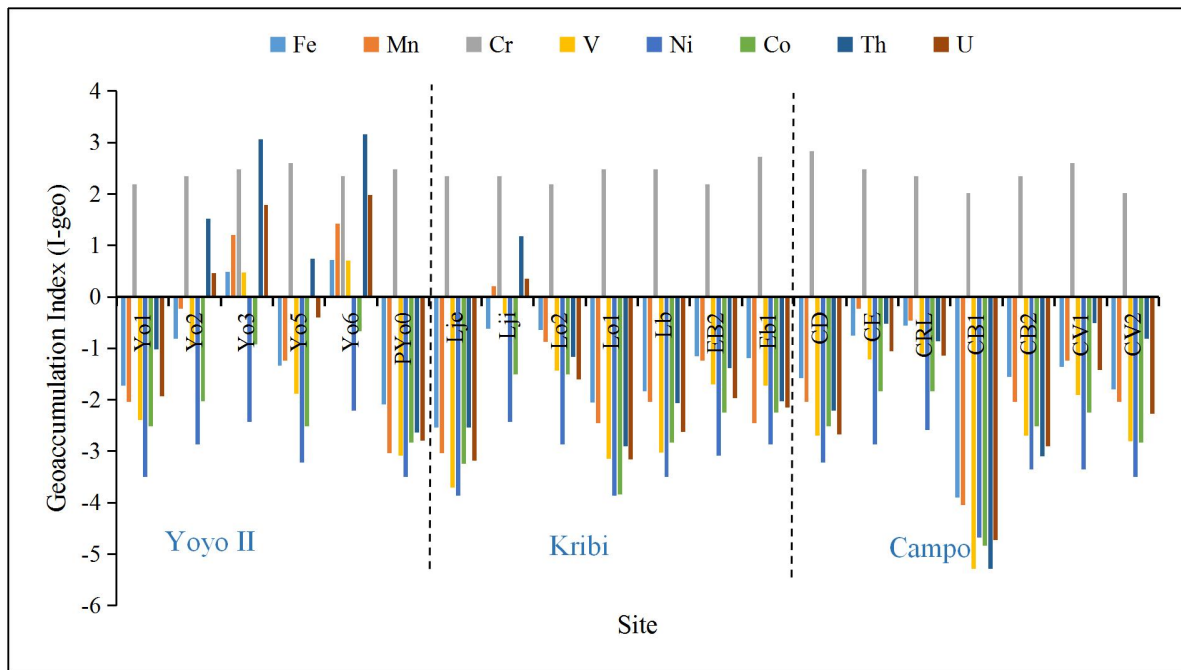


**Figure 2.** Calculation of geoaccumulation indices of different metals and radionuclides in the sediment of southern part of the Cameroonian coast.

### 3.3 Contamination Factor (CF), Degree of Contamination (DC) and Pollution Load Index (PLI)

The contamination factor (CF) was determined using Equation (3). In this study, CF is classified into four classes for the sediment samples from Yoyo II (Table 1; Appendix 2; Figure 3). In the Yoyo II, Fe, V, Ni, and Co have values of  $CF < 1$ , as well as some samples containing Mn, Th, and U. These values suggest that the sediments would be low contamination (Table 1; Figure 3). Uranium, Th, and Mn have samples that mostly fall into the class where CF values vary from 1 to 3 and 3 to 6, meaning that, the sediments are moderate to considerably contaminated. Chromium has values of  $CF > 6$  in all the samples. This is also observed in two samples containing Th. These values indicate a high rate of contamination (Table 1; Figure 3). The locality of Kribi and Campo shows that, in most of the samples studied, all the metals have values of  $CF < 1$ , meaning that these sediments are weakly contaminated, except Cr which has values of  $CF > 6$ , meaning that, the sediments of Kribi and Campo are strongly contaminated with Cr (Appendix 2; Table 1; Figure 3). The low, moderate and considerable contamination of the sediments of the studied samples by these metals would be caused

by the impact of external discontinuous sources such as agricultural runoff, and other anthropogenic contributions such as household waste dumping, tourism and fishing activities. This outcome is consistent with that obtained by Ekoa Bessa et al. [39,25,6] in sediments from the Moloundou swamp, sediments from the coastal areas of Limbé in the northern part of the coastline, and investigated sediments along the coastal zone of Cameroon, respectively. The same result was obtained by Mandeng et al. [12] in sediments of the Abiete-Toko gold district, Southern Cameroon. Moreover, the high Cr contamination is thought to be due to emissions from industry such as sludge combustion and tanneries, and anthropogenic activities such as the frequent use of phosphate fertilizers on soils. The degree of contamination (DC) values range between (9.48-37.13) for the Yoyo II station; (8.84-17.62) for the Kribi station and (6.52-13.56) for the Campo station. DC values obtained in the studied sediments show that these sediments have a moderate, considerable and high degree of contamination ( $8 \leq DC < 32$  and  $DC > 32$ ). The results from each station are presented and observed in (Appendix 2; Figure 4). These results confirm those obtained on the CF, this could be due to the anthropogenic inputs, industrial activities, soil leaching and agricultural runoff.

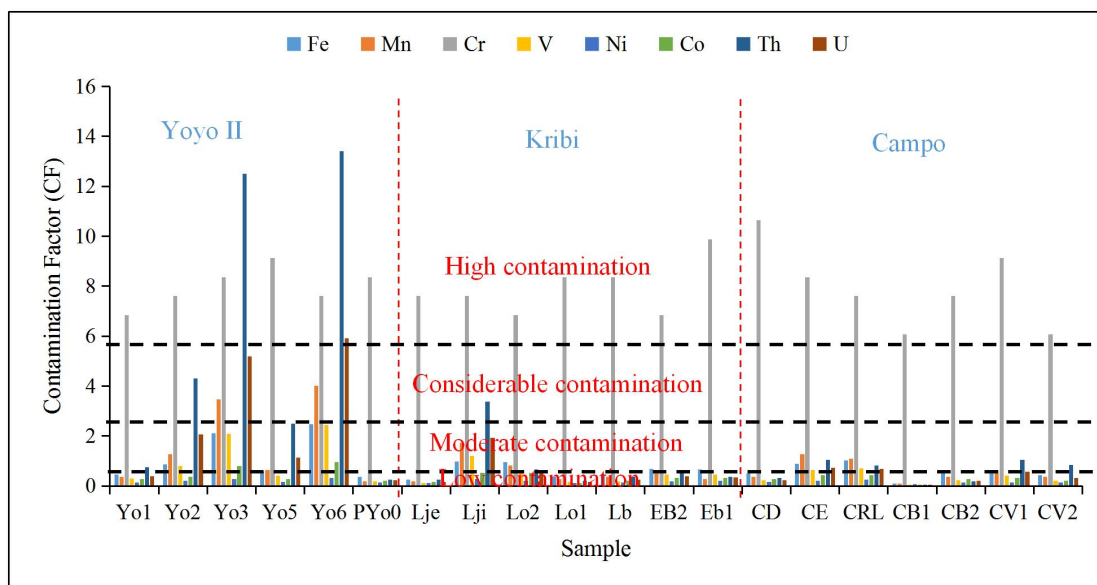


**Figure 3.** Contamination factors of different metals and radionuclides in the sediment of southern part of the Cameroonian coast.

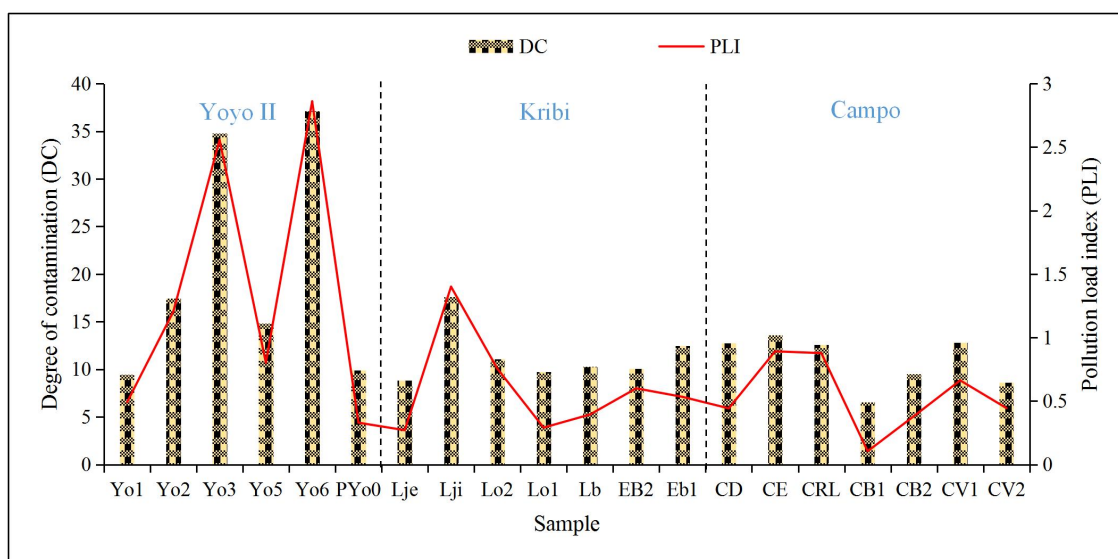


**Figure 4.** Degree of contamination (DC) and pollution load index (PLI) of metals and radionuclides of southern part of the Cameroonian coast.

The pollution load index (PLI) was calculated from Equation (4) for the sediment samples in this study, and their spatial distribution is shown in Figure 4. Appendix 2 gives a summary of the calculated values of the selected analyzed metals. The PLI values in all sampling stations are less than 1 and the sediments are classified as unpolluted, except at the Yoyo II station which shows that 50% of the samples from this station are contaminated with metals to some degree. The PLI in this study is very low when compared to other coastal environments reported by Ekoa Bessa et al. [25], and Sankarappan et al. [35]. While

the high values recorded in these sediments are similar to those collected in the sediments of Moloundou Swamp, eastern Cameroon [39], as well as those of the Lobé River in Cameroon [5].

### 3.4 Assessment of Potential Ecological Risk

Beyond the assessment of heavy metal concentrations, an ecological assessment of heavy metals is required to understand potential harmful effects. The results of the potential ecological risk factor (Er) and the potential ecological risk index (RI) of heavy metals of the three stations



studied along the Southern part of the Cameroonian coast are given in Appendix 3 and Figure 5. The Er of the three stations (Yoyo II, Kribi and Campo) showed a low potential ecological risk factor ( $Er < 40$ ) for the trio Mn, Cr and Ni (Table 1, Appendix 3 and Figure 5). The RI of heavy metals studied in the sediments of three stations showed a low index of ecological risk. In general, in the sediments of this southern part of Cameroonian coast, the possible ecological evaluation (Er and RI) of heavy metals trends to  $Cr > Mn > Ni$ . The study region is a low risk zone, according to the ecological risk assessment, which could be due to anthropogenic activities and which could affect the concentration of heavy metals. These results are in agreement with those of several authors, in particular the results obtained by El-Amier et al. [18], in the sediments of Mediterranean Sea Drain Estuaries in Egypt; those obtained by Ekoa Bessa et al. [25], in the beach sediments along the Atlantic Ocean (Limbe costal fringes, Cameroon) and those obtained by Mandeng et al. [12], in the sediments of

Abiete-Toko gold district, southern Cameroon.

### 3.5 Statistical Analysis

A Pearson correlation analysis was realized using COS-TAT 6.3 software. The correlation coefficient values of this study are listed in Table 3. Pearson correlation indicates that the Fe concentration was significantly positive, correlated ( $p < 0.01$ ) with Mn, V, Co (0.98), U (0.94), Th (0.93), Ni (0.89). However, several elements such as Co, Th and U had significant positive correlations ( $p < 0.01$ ) with V (0.96), Mn (0.95), Ni (0.93); Mn (0.96), Co (0.87), Ni (0.73) and Mn (0.98), V (0.97), Co (0.89), Ni (0.77), respectively. A positive relationship between Co, Mn and Ni demonstrated a characteristic natural origin of these components in the sediments while good correlation between each other could suggest the important activity from anthropogenic sources, and that they can be affected by possible additions [5].

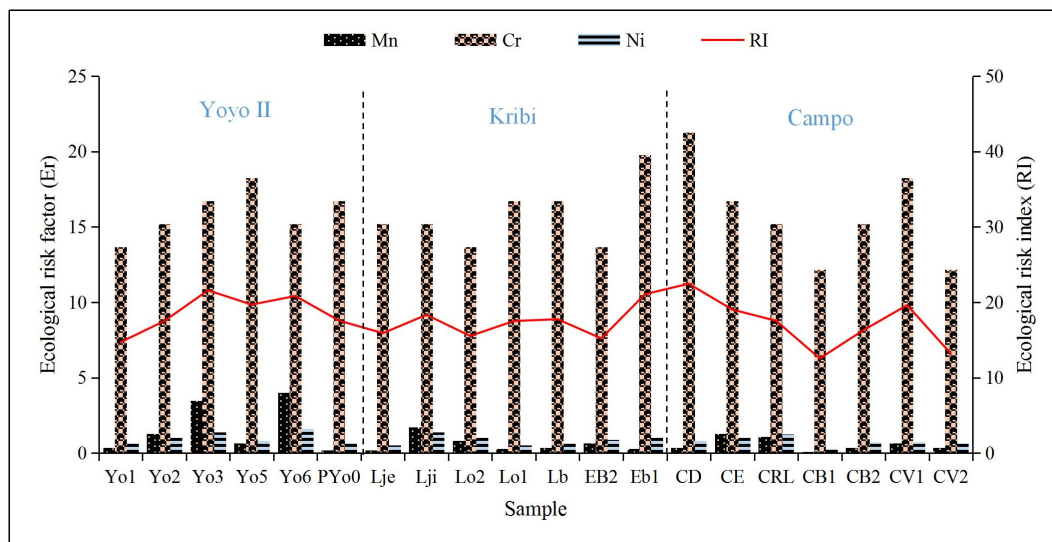


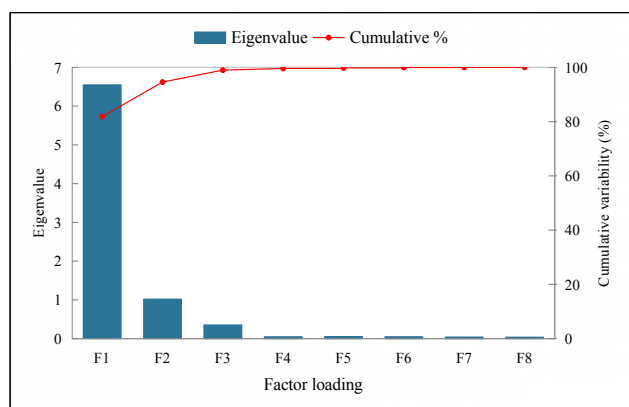
Figure 5. Calculation of potential factor index (Eri) and potential ecological risk index (RI) in sediments from sampling stations along the southern part of the Cameroonian coast.

Table 3. Pearson correlation.

Elements	Fe	Mn	Cr	V	Ni	Co	Th	U
Fe	1							
Mn	0.98	1						
Cr	0.03	-0.02	1					
V	0.983	0.99	0.00	1				
Ni	0.893	0.85	0.12	0.88	1			
Co	0.98	0.95	0.02	0.96	0.93	1		
Th	0.93	0.96	0.00	0.96	0.73	0.87	1	
U	0.94	0.98	0.01	0.97	0.77	0.89	1.00	1

Correlation is significant at  $p < 0.05$ .

To better comprehend the link between these variables and determine their origin, principal components analysis was performed on sediment characteristics and heavy metals. The first two main components with eigenvalues greater than 1 account for 94.57% of the total variance, as illustrated in supplemental Appendix 4 and Figure 6. As a result, these two components play an important role in explaining heavy metal contaminations and their source in the studied area.



**Figure 6.** Scree plot, eigenvalue and variance of principal components.

The results revealed that the first main component (F1) accounted for 81.83% of total variation, with substantial loadings encompassing all of the factors tested (Figure 7a). The existence of Fe in the same components indicates that all elements are positively associated to this group, which could imply that these elements have a natural origin. The second principal component (F2) accounted for 12.27% of total variance (Figure 7a). This group shows an absence of anthropogenic and natural activity. Chromium, Ni and Co are derived from the terrigenous detrital matter carried by runoff and the lithological features of the drainage area Wang et al. [43], Chougong et al. [5]. This finding suggests that this group is likely to be an anthropogenic factor.

Cluster analysis is a technique for gaining valuable insight into the grouping of data based on similarity. The cluster analysis of the sediments stations by metals and radionuclides showed very similar tendencies in this study, with three separate clusters (C1-C3) (Figure 7b), each consisting of similar studies spread throughout these three stations. The cluster model indicates that the similarity index of cluster sampling sites is as follows: C1 to C3. Class C1 is composed of samples from the three stations, but it is more represented by the samples from Yoyo II and Kribi stations. Class C2 mainly represents samples from Campo and Kribi stations, while class C3 mostly represents the samples from Campo (Figure 7b). Within both class C1,

the stations have more than 50% similarity, class C2 has 35% similarity, and class C3 has 15% similarity. These results show that the different metals obtained are probably influenced by anthropogenic factors and natural sources such as the weathering and erosion of nearby rocks.

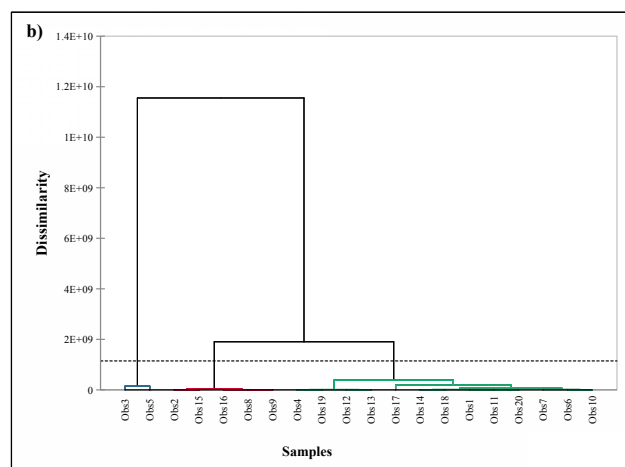
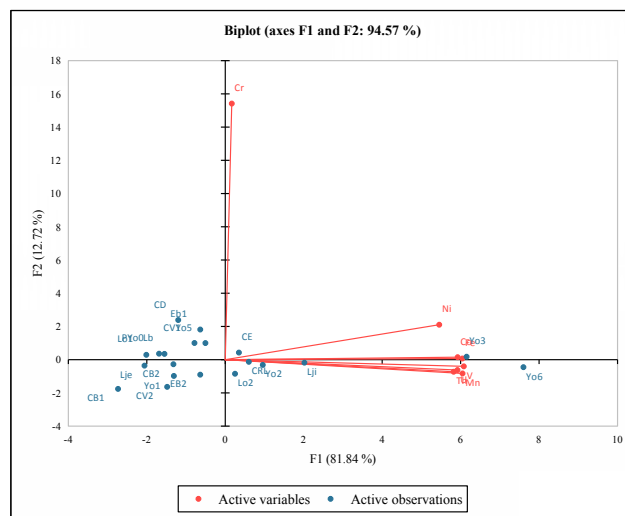


**Figure 7.** Statistical analysis of sampling stations according to heavy metals and radionuclides of sediment samples along the Cameroonian coast a) Principal component analysis (PCA) b) Similarity dendrogram.

## 4. Conclusions

Sediment samples along the southern part of the Cameroonian coast have been investigated to infer the distribution, assessment of pollution and ecological risk of heavy metals (Fe, Mn, Cr, V, Ni and Co), and radionuclides (Th and U). The results of this study showed that all metals, including radionuclides are higher than the average shales values, except Ni and Co, which have lower values. Moreover, the spatial distribution of these elements showed that Fe, Mn, Cr and V have very high concentrations compared

to the others.

The Igeo values of all metals and radionuclides of the study area characterize the sediments unpolluted and moderately polluted, except Cr which presents strongly polluted. The occurrence of Cr in this study could be attributed to the anthropogenic source such as combustion of plastic trash, various agricultural wastes, tourism-related sludge dredging. In general, the assessment of pollution (CF, DC and PLI), in the sediments of the southern part of the Cameroonian coast reveals that these sediments are low to high contaminated, according to each station. These results reveal that these sediments are unpolluted.

The evaluation of the potential ecological risk (Er and RI), indicates that this part of the coast of Cameroon is a low risk area. Matrix correlation, principal components and cluster analysis were employed to confirm the similarity between heavy metals and radionuclides, and to assess the influence of anthropogenic activities on sediment quality. Based on these analyses, heavy metals (Fe, Mn, Cr, V, Ni, and Co) have common anthropogenic sources, while radionuclides (Th and U) have a natural source.

This study provides information on environmental pollution in the study area by assessing the contamination of sediments along the southern of the Cameroonian coast which could be useful to the government in limiting the spread of harmful contaminants.

### Author Contributions

All the authors quoted in this paper have participated ardently in the writing of this manuscript, by exposing very beneficial arguments in the context of this study and have also worked for the form and the linguistic quality provide in this document. work of the first author and will also be used under abstract form for publication of article, and we consent to its use in this manner. We agree with the statements above and declare that this submission follows the policies of the journal as outlined in the guide.

### Funding

AZEB testifies on behalf of all the authors of this paper that, this research has not received any specific grant from any funding body in the public, commercial or non-profit sectors.

### Acknowledgments

The authors are grateful to the Department of Earth Sciences, Faculty of Sciences, University of Dchang.

### Data Availability Statement

All data used in this study have been reported in Table

2 and analyzed in the commercial laboratory ALS from Vancouver, Canada. We add that no additional data was carried out for the realization of this work.

### Conflict of Interest

In the name of all the authors, the corresponding author states that there is no conflict of interest.

### References

- [1] Akcil, A., Erust, C., Ozdemiroglu, S., et al., 2015. A review of approaches and techniques used in aquatic contaminated sediments: metal removal and stabilization by chemical and biotechnological processes. *Journal of Cleaner Production*. 86, 24-36.
- [2] Ip, C.C., Li, X.D., Zhang, G., et al., 2007. Trace metal distribution in sediments of the Pearl River Estuary and the surrounding coastal area, South China. *Environmental Pollution*. 147, 311-323.
- [3] Huang, F., Xu, Y., Tan, Z., et al., 2018. Assessment of pollution and identification of sources of heavy metals in sediments from west coast of Shenzhen, China. *Environmental Sciences and Pollution Research*. 25, 3647-3656.
- [4] Bramha, S.N., Mohanty, A.K., Satpathy, K.K., et al., 2014. Heavy metal content in the beach sediment with respect to contamination levels and sediment quality guidelines: A study at Kalpakkam coast, southeast coast of India. *Environment Earth Sciences*. 72, 4463-4472.
- [5] Chougong, D.T., Nguetchoa, G., Dicka, E.H., et al., 2021. Distributions of trace metals and radionuclides contamination in alluvial sediments from the Lobé River in Cameroon. *Earth System and Environment*. 6(1), 121-139.
- [6] Ekoa Bessa, A.Z., Ambassa Bela, V., Nguetchoa, G., et al., 2022. Characteristics and source identification of environmental trace metals in beach sediments along the Littoral zone of Cameroon. *Earth Systems and Environment*. 6, 175-187.
- [7] Bastami, K.D., Neyestani, M.R., Shemirani, F., et al., 2015. Heavy metal pollution assessment in relation to sediment properties in the coastal sediments of the southern Caspian Sea. *Marine Pollution Bulletin*. 92, 237-243.
- [8] Zhang, H., Walker, T.R., Davis, E., et al., 2019. Spatiotemporal characterization of metals in small craft harbor sediments in Nova Scotia, Canada. *Marine Pollution Bulletin*. 140, 493-502.
- [9] Li, F., Huang, J., Zeng, G., et al., 2013. Spatial risk assessment and sources identification of heavy met-

- als in surface sediments from the Dongting Lake, Middle China. *Journal of Geochemical Exploration*. 132, 75-83.
- [10] Hossain, M.B., Shanta, T.B., Ahmed, A.S., et al., 2019. Baseline study of heavy metal contamination in the Sangu River estuary, Chattogram, Bangladesh. *Marine Pollution Bulletin*. 140, 255-261.
- [11] Bartlett, J.H., Castro, A., 2019. Isotopic spectroscopy of uranium atomic beams produced by thermal reduction of uranium compounds. *Spectrochimica Acta part B: Atomic Spectroscopy*. 155, 61-66.
- [12] Mandeng, E.P.B., Bidjeck, L.M.B., Bessa, A.Z.E., et al., 2019. Contamination and risk assessment of heavy metals, and uranium of sediments in two watersheds in Abiete-Toko gold district, Southern Cameroon. *Heliyon*. 5, 02591.
- [13] Baranov, V.I., Morozova, N.G., 1971. The behavior of natural radionuclides in soils. *Radioekologiya*. 2, 13-41.
- [14] Armstrong-Altrin, J.S., 2020. Detrital zircon U-Pb geochronology and geochemistry of the Riachuelos and Palma Sola beach sediments, Veracruz State, Gulf of Mexico: A new insight on palaeoenvironment. *Journal of Palaeogeography*. 9, 1-27.
- [15] Tehna, N., Sababa, E., Ekoa Bessa, A.Z., et al., 2019. Mine waste and heavy metal pollution in Betare-Oya Mining Area (Eastern Cameroon). *Environmental and Earth Sciences Research Journal*. 6, 167-176.
- [16] Noa Tang, D., Ekoa Bessa, A.Z., Brice, T.K., et al., 2021. Heavy metal contamination and ecological risk assessment of overlying water and sediments of Nkozoa Lake (Southern Cameroon). *Annual Research and Review Biology*. 92-109.  
DOI: <https://doi.org/10.9734/arrb/2021/v36i430366>
- [17] Bianchini, A., Cento, F., Guzzini, A., et al., 2019. Sediment management in coastal infrastructures: Techno-economic and environmental impact assessment of alternative technologies to dredging. *Journal of Environmental Management*. 248, 109332.
- [18] El-Amier, Y.A., Bessa, A.Z.E., Elsayed, A., et al., 2021. Assessment of the heavy metals pollution and ecological risk in sediments of Mediterranean Sea Drain Estuaries in Egypt and Phytoremediation potential of two emergent plants. *Sustainability*. 13, 12244.
- [19] Bilong, P., Belinga, S.E., Volkoff, B., 1992. Sequence of evolution of armoured landscapes and ferrallitic soils in tropical forest areas of Central Africa: Place of soils with spotted clay horizons. *Comptes Rendus de l'Academie des Sciences*. 314, 109-115.
- [20] Nguetchoua, G., Bessa, A.Z., Eyong, J.T., et al., 2019. Geochemistry of cretaceous fine-grained siliciclastic rocks from Upper Mundeck and Logbadjeck Formations, Douala sub-basin, SW Cameroon: Implications for weathering intensity, provenance, paleoclimate, redox condition, and tectonic setting. *Journal of African Earth Sciences*. 152, 215-236.
- [21] Mbesse, C.O., Bessong, M., Ntamak-Nida, M.J., et al., 2020. Palynology and palynofacies analyses in the Douala sub-basin: Implications on palaeoenvironment evolution of the Souellaba Formation/west Cameroon. *Journal of African Earth Sciences*. 172, 104004.
- [22] Nguene, F.R., Tamfu, S., Loule, J.P., et al., 1992. Palaeoenvironments of the Douala and Kribi/Campo subbasins in Cameroon, West Africa. *Bulletin des Centres de recherches exploration-production Elf-Aquitaine. Mémoire*. (13), 129-139.
- [23] Lawrence, R.S., Munday, S., Bray, R., 2002. Regional geology and geophysics of the Eastern Gulf of Guinea (Niger Delta to Rio Muni). *Lead Edge*. 21, 1112-1117.
- [24] Ntamak-Nida, M.J., Bourquin, S., Makong, J.C., et al., 2010. Sedimentology and sequence stratigraphy from outcrops of the Kribi-Campo subbasin: Lower Mundeck Formation (Lower Cretaceous, southern Cameroon). *Journal of African Earth Sciences*. 58, 1-8.
- [25] Ekoa Bessa, A.Z., Nguetchoua, G., Janpou, A.K., et al., 2021. Heavy metal contamination and its ecological risks in the beach sediments along the Atlantic Ocean (Limbe coastal fringes, Cameroon). *Earth System and Environment*. 5, 433-444.
- [26] Chen, H.Y., Teng, Y.G., Wang, J.S., et al., 2012. A framework for pollution characteristic assessment and source apportionment of heavy metal contaminants in riverbed sediments: A case study. *Fresenius Environmental Bulletin*. 21, 1112-1119.
- [27] Singovszka, E., Balintova, M., 2019. Enrichment factor and geo-accumulation index of trace metals in sediments in the River Hornad, Slovakia. *IOP Conference Series: Earth and Environmental Science*. 222, 012023.
- [28] Tomlinson, D., Wilson, J., Harris, C., et al., 1980. Problems in the assessment of heavy-metal levels in estuaries and the formation of a pollution index. *Helgoländer Meeresuntersuchungen*. 33, 566-575.
- [29] Håkanson, L., 1980. An ecological risk index for aquatic pollution control. A sedimentological approach. *Water Research*. 14, 975-1001.
- [30] Wang, J., Jiang, Y., Sun, J., et al., 2020. Geochemical transfer of cadmium in river sediments near a lead-zinc smelter. *Ecotoxicology and Environmental Safety*. 196, 110529.
- [31] Suresh, G., Ramasamy, V., Meenakshisundaram, V., et al., 2011. Influence of mineralogical and heavy

- metal composition on natural radionuclide concentrations in the river sediments. *Applied Radiation and Isotopes*. 69, 466-1474.
- [32] Turekian, K.K., Wedepohl, K.H., 1961. Distribution of the elements in some major units of the earth's crust. *Geological Society America Bulletin*. 72, 175-192.
- [33] Ramos-Vázquez, M.A., Armstrong-Altrin, J.S., 2019. Sediment chemistry and detrital zircon record in the Bosque and Paseo del Mar coastal areas from the southwestern Gulf of Mexico. *Marine and Petroleum Geology*. 110, 650-675.
- [34] Saifullah, S.M., Ismail, S., Khan, S.H., et al., 2004. Land use-iron pollution in mangrove habitat of Karachi, Indus Delta. *Earth Interactions*. 8, 1-9.
- [35] Sankarappan, R., Gopalakrishnan, G., Shanmugam, R., et al., 2021. Diffusion, textural characteristics, and source identification of the heavy metals in the Karankadu mangrove sediments, South India. *Arabian Journal of Geosciences*. 14, 1.
- [36] Long, E.R., Field, L.J., Macdonald, D.D., 1998. Predicting toxicity in marine sediments with numerical sediment quality guidelines. *Environmental Toxicology and Chemistry*. 17, 714-727.
- [37] Kasilingam, K., Gandhi, M.S., Krishnakumar, S., et al., 2016. Trace element concentration in surface sediments of Palk Strait, southeast coast of Tamil Nadu, India. *Marine Pollution Bulletin*. 111, 500-508.
- [38] Li, C., Chengwen, S., Yanyan, Y., et al., 2015. Spatial distribution and risk assessment of heavy metals in sediments of Shuangtaizi estuary, China. *Marine Pollution Bulletin*. 98, 358-364.
- [39] Ekoa Bessa, A.Z., El-Amier, Y.A., Doumo, E.P.E., et al., 2018. Assessment of sediments pollution by trace metals in the Moloundou swamp, southeast Cameroon. *Annual Research and Review Biology*. 1-13.
- [40] Sahoo, S.K., Hosoda, M., Kamagata, S., et al., 2011. Thorium, uranium and rare earth elements concentration in weathered Japanese soil. *Samples Progress in Nuclear Science and Technology*. 1, 416-419.
- [41] Domingo, J.L., 2001. Reproductive and developmental toxicity of natural and depleted uranium: A review. *Reproductive Toxicology*. 15, 603-609.
- [42] Pinto, M.M.S.C., Silva, M.M.V.G., Neiva, A.M.R., 2004. Pollution of water and stream sediments associated with the Vale De Abrutiga Uranium Mine, Central Portugal Mine. *Water and the Environment*. 23, 66-75.
- [43] Wang, X., Chen, F., Hasi, E., et al., 2008. Desertification in China: An assessment. *Earth Sciences Reviews*. 88, 188-206.

## Appendix

**Appendix 1.** Geoaccumulation indices for heavy metals (Fe, Mn, Cr, V, Ni, Co) and radionuclides (Th, U).

ID	Fe	Mn	Cr	V	Ni	Co	Th	U	Station
Yo1	-1.72	-2.04	2.19	-2.40	-3.50	-2.51	-1.02	-1.93	Yoyo II
Yo2	-0.81	-0.23	2.34	-0.93	-2.87	-2.03	1.52	0.46	
Yo3	0.49	1.21	2.48	0.48	-2.42	-0.93	3.06	1.79	
Yo5	-1.33	-1.23	2.60	-1.88	-3.21	-2.51	0.74	-0.40	
Yo6	0.72	1.42	2.34	0.71	-2.21	-0.66	3.16	1.98	
PYo0	-2.09	-3.04	2.48	-3.08	-3.50	-2.83	-2.63	-2.79	
Lje	-2.54	-3.04	2.34	-3.70	-3.87	-3.25	-2.54	-3.19	Kribi
Lji	-0.61	0.21	2.34	-0.32	-2.42	-1.51	1.17	0.36	
Lo2	-0.65	-0.87	2.19	-1.44	-2.87	-1.51	-1.17	-1.61	
Lo1	-2.05	-2.46	2.48	-3.15	-3.87	-3.83	-2.91	-3.16	
Lb	-1.83	-2.04	2.48	-3.02	-3.50	-2.83	-2.07	-2.62	
EB2	-1.15	-1.23	2.19	-1.70	-3.09	-2.25	-1.38	-1.97	
Eb1	-1.19	-2.46	2.72	-1.72	-2.87	-2.25	-2.03	-2.15	Campo
CD	-1.58	-2.04	2.83	-2.70	-3.21	-2.51	-2.21	-2.67	
CE	-0.76	-0.23	2.48	-1.22	-2.87	-1.83	-0.53	-1.06	
CRL	-0.55	-0.46	2.34	-1.10	-2.58	-1.83	-0.86	-1.14	
CB1	-3.90	-4.04	2.02	-5.29	-4.67	-4.83	-5.29	-4.72	
CB2	-1.55	-2.04	2.34	-2.70	-3.35	-2.51	-3.10	-2.91	
CV1	-1.37	-1.23	2.60	-1.91	-3.35	-2.25	-0.51	-1.42	
CV2	-1.80	-2.04	2.02	-2.80	-3.50	-2.83	-0.82	-2.27	

**Appendix 2.** Statistical descriptive of contamination factor (CF), degree of contamination (DC) and pollution load index (PLI) in the sediment samples.

ID	CF								DC	PLI	Station
	Fe	Mn	Cr	V	Ni	Co	Th	U			
Yo1	0.45	0.36	6.84	0.28	0.13	0.26	0.74	0.39	9.48	0.49	Yoyo II
Yo2	0.85	1.28	7.60	0.78	0.21	0.37	4.31	2.07	17.47	1.20	
Yo3	2.10	3.46	8.36	2.09	0.28	0.79	12.50	5.19	34.78	2.56	
Yo5	0.60	0.64	9.12	0.41	0.16	0.26	2.50	1.14	14.82	0.80	
Yo6	2.47	4.01	7.60	2.45	0.32	0.95	13.42	5.92	37.13	2.86	
PYo0	0.35	0.18	8.36	0.18	0.13	0.21	0.24	0.22	9.88	0.33	
Lje	0.26	0.18	7.60	0.12	0.10	0.16	0.26	0.16	8.84	0.27	Kribi
Lji	0.98	1.73	7.60	1.20	0.28	0.53	3.38	1.92	17.62	1.40	
Lo2	0.96	0.82	6.84	0.55	0.21	0.53	0.67	0.49	11.06	0.76	
Lo1	0.36	0.27	8.36	0.17	0.10	0.11	0.20	0.17	9.74	0.29	
Lb	0.42	0.36	8.36	0.18	0.13	0.21	0.36	0.24	10.28	0.39	
EB2	0.67	0.64	6.84	0.46	0.18	0.32	0.58	0.38	10.07	0.60	
Eb1	0.66	0.27	9.88	0.45	0.21	0.32	0.37	0.34	12.49	0.53	Campo
CD	0.50	0.36	10.64	0.23	0.16	0.26	0.33	0.24	12.73	0.44	
CE	0.89	1.28	8.36	0.65	0.21	0.42	1.04	0.72	13.56	0.89	
CRL	1.02	1.09	7.60	0.70	0.25	0.42	0.83	0.68	12.59	0.88	
CB1	0.10	0.09	6.08	0.04	0.06	0.05	0.04	0.06	6.52	0.10	
CB2	0.51	0.36	7.60	0.23	0.15	0.26	0.18	0.20	9.50	0.38	
CV1	0.58	0.64	9.12	0.40	0.15	0.32	1.05	0.56	12.82	0.66	CV2
CV2	0.43	0.36	6.08	0.22	0.13	0.21	0.85	0.31	8.60	0.44	

**Appendix 3.** Pollution indices (Er and RI) in the sediment study.

ID	Mn	Cr	Ni	RI	Station
Yo1	0.36	13.68	0.66	14.71	YOYO II
Yo2	1.28	15.20	1.03	17.51	
Yo3	3.47	16.72	1.40	21.58	
Yo5	0.64	18.25	0.81	19.69	
Yo6	4.01	15.20	1.61	20.83	
PYo0	0.18	16.72	0.66	17.57	
Lje	0.18	15.20	0.51	15.90	Kribi
Lji	1.73	15.20	1.40	18.33	
Lo2	0.82	13.68	1.03	15.53	
Lo1	0.27	16.72	0.51	17.51	
Lb	0.36	16.72	0.66	17.75	
EB2	0.64	13.68	0.88	15.20	
Eb1	0.27	19.77	1.03	21.07	Campo
CD	0.36	21.29	0.81	22.46	
CE	1.28	16.72	1.03	19.03	
CRL	1.09	15.20	1.25	17.55	
CB1	0.09	12.16	0.29	12.55	
CB2	0.36	15.20	0.74	16.30	
CV1	0.64	18.25	0.73	19.62	CV2
CV2	0.36	12.16	0.66	13.19	

**Appendix 4.** Rotated component matrix of heavy metals and radionuclides.

<b>Factor loading</b>	<b>F1</b>	<b>F2</b>	<b>F3</b>	<b>F4</b>	<b>F5</b>
Fe	0.387	0.005	0.069	0.458	0.098
Mn	0.387	-0.053	-0.110	-0.010	0.750
Cr	0.011	0.987	-0.143	0.046	0.041
V	0.389	-0.026	-0.035	-0.184	0.255
Ni	0.349	0.135	0.689	-0.553	-0.158
Co	0.379	0.010	0.315	0.610	-0.320
Th	0.373	-0.046	-0.488	-0.124	-0.404
U	0.379	-0.040	-0.388	-0.247	-0.266
Eigenvalue	6.548	1.018	0.353	0.048	0.016
Variability (%)	81.844	12.723	4.413	0.601	0.206
Cumulative (%)	81.844	94.568	98.981	99.582	99.788